Effect of Calcination Temperature on Silica-Asphalt Composite Properties using Amorphous Rice Husk Silica

S. Sembiring[1], A. Riyanto[1], I. Firdaus[1], Junaidi[1], R. Situmeang[2]

[1] Department of Physics, Faculty of Mathematics and Natural Sciences, Lampung University, Street Prof. Soemantri Brojonegoro, No 1 Bandar Lampung, 35145, Indonesia
[2] Department of Chemistry, Faculty of Mathematics and Natural Sciences, Lampung University, Street Prof. Soemantri Brojonegoro, No 1 Bandar Lampung, 35145, Indonesia

Email : simon.sembiring@fmipa.unila.ac.id[1]

Abstract. This study aims to investigate the effect of thermal treatment on the phase formation and physical characteristics of silica asphalt composite prepared from rice husk silica and asphalt powders. The mass ratio of asphalt to silica is 1:2, and subjected to calcining temperatures of 200-450 °C. Development of structures was characterized using X-ray diffraction (XRD), Fourier Transform Infrared (FTIR) spectroscopy and scanning electron microscopy (SEM). Further evaluation was made by comparing the characteristics of the silica-asphalt composite include the density, porosity, and compressive strength. The XRD study revealed that the major phases were carbon and silica amorphous, The XRD study revealed that the major phases were silica and carbon amorphous, which were associated with are Si-OH, Si-O-Si and C-H functional groups according to FTIR analysis. In addition, an increased calcination temperatures was followed by an increase in the density and compressive strength. Based on these characteristics, the samples are considered for the roof material, suggesting their potential use in substitute lightweight steel roof devices.

Keyword: Rice husk, Silica, Asphalt, Microstructure, Structure, Thermal

1. Introduction

Asphalt/bitumen is a natural polymer of low molecular weight mainly used as a binder, which produced by fractional distillation of crude oil and catalytic cracking of hydrocarbons [1]. Asphalt has a chemical composition with unique viscosity, elasticity, waterproof, good adhesive and high impermeability properties. For extending the use of asphalt in various fields such as, road traffic, roofing, sealing, waterproofing agent, coating, and insulation applications, the high-quality modified asphalt and its mixtures has become an important. Therefore, it is imperative to study the composite-modified asphalt mixture to meet the requirements of high flow, heavy load, stability, durability, and high strength. For example when asphalt blended with proportion of polymers used in built up membranes for the roofing industry [2]. Some researchers have tried changing the characteristics of asphalt to improve functionality and benefits by using various polymers such as styrene-butadiene-styrene/SBS [3-4], waste crumb rubber [5-6], used waste rubber and plastic [7-8], waste polyethylene [9-10] and styrene-butadiene rubber/SBR [11]. According to previous studies indicate that modified asphalt is not only stable well at

high and low temperature performance, but also has durability and resistance to deformation cracks [12-13].

One of the an inorganic additives of materials that have been used intensively is silica. Due to the high surface area, and strong adsorption, silica has the potential to prepare asphaltic materials with desirable properties. Rice Husk is an interesting waste material as it has high silica content with quite high levels. According to previous research, the best silica obtained is silica amorphous with high purity [14-15]. Shen, et.al., 2011 [16] reported that active silica is high of rice husks can be produced at low calcination temperatures (800 ° C), while with silica high purity and chemical reactivity were obtained by controlling heating conditions [17]. Recently, there have been studies on the use of various silica particles to modify asphalt binders. For example, silica has been highly used in the polymer industry to reduce aging and to increase mechanical and physical properties of base materials such as stiffness, toughness, strength and thermal stability [18]. Sembiring, et.al., 2019 [19] obtained transformation of asphaltene into silica and carbon, with increased decomposition temperature of asphalt. In addition, an increased silica addition was followed by an increase in the density, compressive strength, swelling thickness, and water absorption, while the opposite was true for the porosity [20]. Chong, et.al., 2012 and Song, et.al., 2011[21-22] found that silica could improve water stability, temperature and fatique performances. They also shown that silica could reduce the air void and improve the indirect tensile strength and indirect tensile stiffness modulus of asphalt composite. With the addition of silica, cohesion and viscosity of asphalt may increase, which are good for high temperature situations [23]. Tan, et.al., 2009 [24] carried out modified asphalt mixture. Their results indicated that the addition of silica fume could improve the low-temperature performance and increase the contraction coefficient of the mixture. Abdutalib, et.al., 2015 [25] also reported that modifiers such as silica fume have the capability to enhance oxidative aging resistance of asphalt and improved temperature performance of asphalt [26].

Recognizing the important roles of asphalt composite in various industrial areas, production of asphalt composite has been continuously explored, and in general, it is found that the characteristic of asphalt composite is strongly dependent on the chemical composition, the types of raw material, and heating temperature. Research on the effect of heating treatment phenomenon on the properties of asphalt composite is very interesting. For example, the effect of heating on asphalt composite can support the self-healing process [27-29] and can increase aging phase, hardness, viscosity and softening temperature of asphalt. Sing, et.al., 2018 [30] found that SBS polymer-modified bitumen decreases elastic recovery, and softening point associated with the resistance to permanent deformation of asphalt composite at a temperature of 210 ^{o}C.

Rice husk as agricultural waste is known to contain large amounts of silica, the authors have used as a ceramic or composite material including, mullite [31], forsterite [32], cordierite [33], silica-asphalt [19-20]. In addition, amorphous silica from rice husk has been used for the preparation of various silica-based materials, such as the production of nano silica [34-36], zeolite [37-38], nano porous carbon [39-40], nepheline [41].

Based on the use of silica from rice husks and asphalt quoted above, it shows that these materials have high potential for use as a raw material for the production of silica-asphalt composites. This potential is the main reason for carrying out this study as an attempt to evaluate the feasibility of this agriculture waste as alternative raw materials for silica asphalt composite production. This work emphasises the effect of thermal treatment on the crystallisation properties of silica asphalt composite. To obtain detailed the mechanism and the microscopic characteristics some modified asphalt characteristics were analysed through FTIR, XRD, FTIR and SEM/EDX. Furthermore, the physical properties of asphalt composites are investigated by measuring the density, porosity, and compressive strength.

2. Experimental

2.1. Materials

Raw husk used as a source of silica was from local rice milling industry in Bandar Lampung Province, Indonesia. The matrix asphalt used in this experiment was obtained from Buton refinery, Southeast Sulawesi Province, Indonesia, and the modifiers were made of rice husk silica. The chemicals used are 5% NaOH 5% KOH, 5% HCl, and absolute alcohol (C2H5OH) purchased from Merck (kGaA, Darmstadt, Germany), and distilled water.

2.2. Preparation of composite-modified asphalt

Rice husk silica was obtained using alkali extraction method following the procedure reported in previous study [32]. In this stage, 50 g dried husk was mixed with 500 ml of 5% KOH solution in a beaker glass, boiled for 30 min, and followed to cool to room temperature and left for 24 h. The mixture was filtered to separate the filtrate which contains silica sol. The sol obtained are dripped with 5% HCl solution until the sol turn completely to the gel. The gel was dried at 110 °C for eight hours and then ground into a powder by mortar and sieved to 200 meshes. Preparation of silica-asphalt composite was carried out by mixing raw materials with the composition of silica : asphalt of 2:1 by mass, in accordance with the composition of silica asphalt as reported in previous studies [20].Typically, 50 g of solid asphalt is melted by heating at 100 °C and mixed with powdered silica using a shear mixer at a rate of 125 rpm for 4 hours. Finally, calculated the quantity of silica is added under stirring to asphalt to provide the silica and asphalt as a mass ratio of 2:1. Furthermore, the powder was pressed in a metal die with the pressure of 2 × 104 N/m2 to produce cylindrical pellet and the pellets were calcined at temperatures of 200, 250, 300, 400, and 450 °C, using temperature programmed with a heating rate of 3 °C/min and holding time of 6 h at peak temperatures has additional information to appear as a footnote, such as a permanent address or to indicate that they are the corresponding author, the footnote should be entered after the surname.

2.3. Characterisation

A collection of XRD data was conducted with an automated Shimadzu XD-610 X-ray diffractometer at the National Agency for Nuclear Energy (BATAN). The XRD data were taken with CuKα radiation (λ=1.5406 nm) at 40 kV and 30 mA in the range of 2θ = 5-80°, with a step size of 0.02, counting time 1s/step and 0.15° receiving slit. The FTIR data were taken with a Perkin Elmer FTIR. The sample was prepared by mixing with KBr of spectroscopy grade. Morphological analysis of the polished and etched samples was carried out by SEM Philips-XL. Thermal analysis was conducted using DTA Merck Setaram Tag 24 S, under the nitrogen atmosphere with a constant heating rate of 3 °C/min, at the temperature range of 30 to 800 °C. Archimedes method was used to measure bulk density and apparent porosity [42]. The compressive strength was determined with three replicates measurement following the ASTM C268-70.

3. Results and discussion

3.1 Basic characteristics of asphalt and silica

In order to study characteristic of silica-asphalt composite, the samples subjected to calcinate treatment at different temperatures were performed by FTIR, XRD, SEM/EDS method. The FTIR spectra of asphalt and silica are shown in Fig. 1 (a-b). Fig. 1a shows the spectrum of asphalt and Fig. 1b shows the pattern of silica. Figure 1a shows clearly the presence of three high peaks at 2931, 1725 and 1432

cm-1, and followed by other peaks at 956, 724, and 696 cm-1. The peaks at 2931 and 1432 cm-1 show the function of the O-H characteristic group of carboxylic acids and C-H from alkanes, while the peak at 1725 show the vibrations of the carbonyl group C = O, as reported in previous studies [19-20]. Others strong peaks were located at 956, 724, and 696 cm-1, which were related to the bending vibrations of C-H in phenyl. For the silica sample (Figure 1b) was characterized by the existence of several absorption bands associated with silica commonly reported in the literature [43-48]. The broad band centred at around 3448 cm-1 regions is attributed to stretching vibration of hydroxyl (-OH) group of silanol (Si-OH). The existence of Si-OH bond is supported by a weak band centred at around 964 cm-1, and the presence of adsorbed water molecules is supported by the absorption band centred at around 1630 cm-1, which is attributed to bending vibration of the O-H bond. The three characteristic bands at 1103 cm-1, 802 and 470 cm-1, which are attributed to asymmetric stretching vibration, symmetric stretching vibration, and bending vibration of the Si-O-Si bond, respectively.

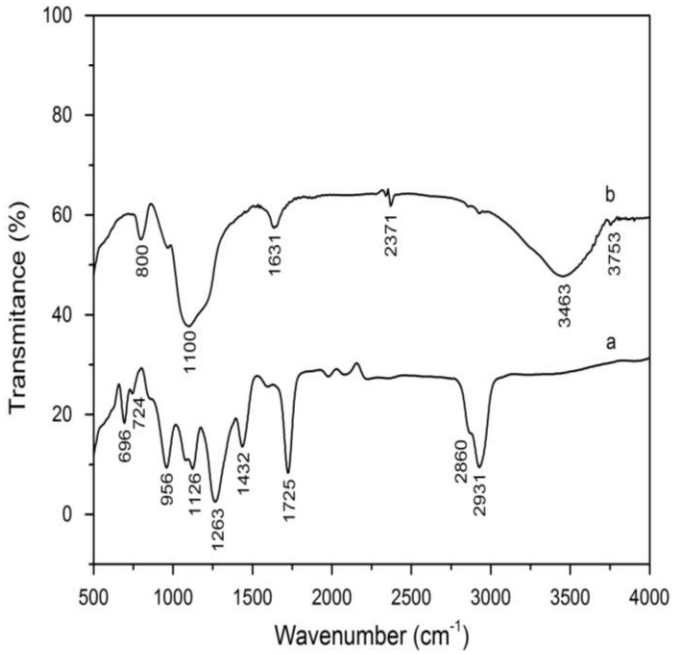

Figure 1. FTIR spectra of samples, (a) asphalt and (b) silica.

3.2 Characteristics of silica-asphalt composite

Figures 2 (a-d) show the spectra of the silica-asphalt samples with the different calcination temperature. Similarly, the diffraction peak intensities of the samples with the different calcination temperature were found to be 10 and 21.8° (Figures 2a-d), amorphously indicating the background intensities from the carbon and silica.

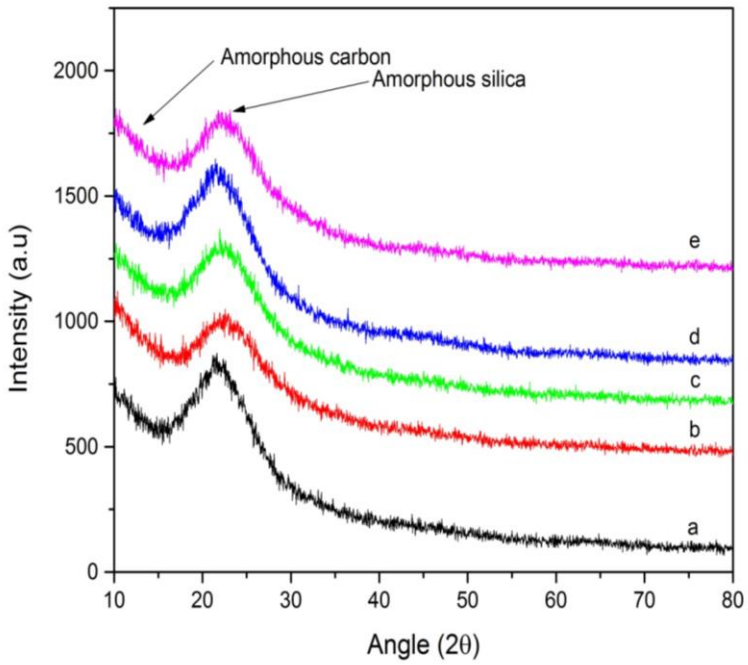

Figure 2. The X-ray diffraction patterns of the samples with the different calcination temperatures using CuKa radiation, (a) (a) 200 ^{o}C, (b) 250 ^{o}C., (c) 300 ^{o}C., (d) 400 ^{o}C and (e) 450 ^{o}C

The presence of an amorphous phase is presumably indicative of the silica and carbon accumulating on the surface. However, the change in the peak diffraction is a result of strong molecular interactions between the asphalt and the silica through the exfoliation and intercalation process in the samples. This may indicate that there are many interactions in the form of crystallisation that do not separate the asphaltene molecules outside their range of London attractions between the silica and asphalt. This result also shows that the intercalation and peeling occur as evidenced by the modified asphalt peaks falling between the two peaks associated with the carbon and silica. This, in turn, suggests an increasing layer distance due to the modification. The diffraction patterns in Fig 1(b-d) indicate that the samples with with increasing the temperature of calcination were still amorphous, marked by the existence of two broad peaks, most likely resulted from accumulation of carbon peak position ($2\theta = 10°$) and silica peak position ($2\theta = 21.8°$).The presence of carbon and silica is in accordance with the results of EDX analyses, described in the following section.

The results of infrared spectra analysis of silica-asphalt samples undergoing calcination treatment at different temperatures are shown in Figure 3 (a-d). As can be seen, wide and weak peak located at around 3448 cm^{-1} (Figure 3a) is generally associated with stretching vibrations of the hydroxyl (-OH) silanol (Si-OH) group and supported by the appearance of absorption at 470 cm-1 and strong bond that is located at 1102 cm^{-1} is associated with asymmetric stretching vibrations from Si-O-Si. Other observed weak bonds located at 2940 and 1474 cm^{-1} may show the characteristic group functionality of O-H from carboxylic acids [49-50 and C-H from alkanes [51-52].

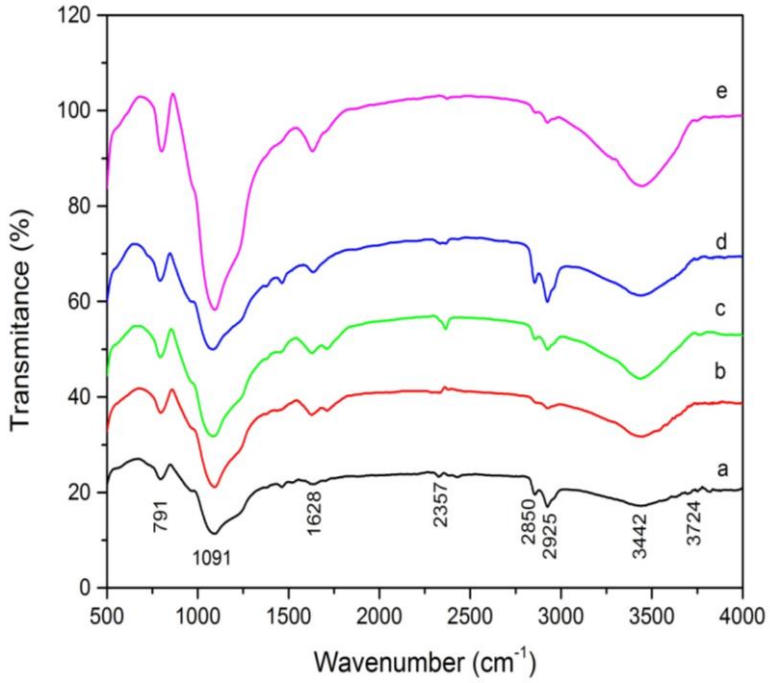

Figure 3. The FTIR spectra of the samples with the different calcination temperatures, (a) (a) 200ºC, (b) 250ºC., (c) 300ºC., (d) 400ºC and (e) 450ºC

Fig 3 (b-e) indicates the significant effect of thermal treatments on the functionality of the samples. The most obvious change is the increase of peaks associated with Si (OH), O-H, and Si-O-Si bonds, indicating the decomposition of asphalt in the surface during heating process. In addition, the intensity of the band assigned to O-H and Si-O-Si bonds increased due to the evaporation of carbon through asphaltene decomposition and silica crystallization. As a consequence, the intensity of the absorption band at 470 and 1102 cm^{-1}, assigned to Si–O–Si vibration increased. Besides, the comparison of peak positions samples from calcination temperature of 250 to 400 ºC indicates that there are no significant chemical change of functional group and bands and the samples are considered as thermal stable under these conditions. In addition, the absorption peak in the all infrared spectra at 2350 cm^{-1} corresponds to the asymmetrical stretch of CO_2. Based on the results of the chemical bond analysis, the increased temperature of calcination shows the peak chemical bond change of the silica asphalt. The most obvious change is the decrease of peak associated with C-H from alkanes. Also, it can be informed that the asphalt undergoes changes between its bonds and the silica. The peaks at 2925 cm^{-1} and 2850 cm are due to C-H vibrations which are caused by the asphalt binder. The significant influences are the emergence of a weak vibration of O-H produced from silanol in Si (OH), at around 3442 cm^{-1}, which indicates the reaction between silica and asphalt during the thermal treatment. It can be seen that there is an obvious difference in the spectrum of silica asphalt sample (Figure 3a) when compared with spectrum of the silica asphalt in Figure 3(b). The exposure to high temperature of calcination (250°C) might change the interactions of silica-asphalt matrix and the embedded thermochromic particles. As can be seen in Figure 3b shows that vibration of O-H increased with increasing the temperature of calcination. Furthermore, the appearance of $Si(OH)_4$ is shown in the absorption wave number 1091 cm^{-1}(Figure 3a), which indicates that the Si–O–Si bond formed by the deformation of the Si-O vibration. The similar bands of Si-O-Si are found exposed up to 400º, while vibration of Si-O-Si increased with increasing temperature treatment of 450ºC.The presence of SiO vibration is observed in the results, showing the strong asphaltene decomposition and silica crystallization.

The surface images and elemental composition of the samples with the different temperature of calcination obtained from SEM and EDS analyses are shown in Fig. 4(a-e) and Table 1. The micrographs

presented in Fig 4(a-e) show significant effect of heating on the size and distribution of the particles on the surface. As shown in Fig 4(a-e), the surfaces morphologies of the samples are marked by the existence of particles with different grain sizes and distribution. The sample with temperature calcination of 200 ^{o}C (Fig 4a) is found by the presence of clusters with different grain sizes and distribution associated to microcracks, and the presence of the major element of carbon (C) oxygen (O), silicon (Si), together with minor element of sulphur (S) and sodium (Na) (Table 1). The clusters are most likely composed of C, while the fine grains are Si and S respectively. The presence of carbon due to the effects of simultaneous heating followed by carbon formation began to form and distributed to cover silica on the surface of the sample, which was marked most likely formed from the arrangement of asphalt structures with the amount (50.96%) C and 7.63% Si (Table 1). According to the leading particles are most likely the carbon present as larger particles, indicating that the sample is dominated by the carbon.

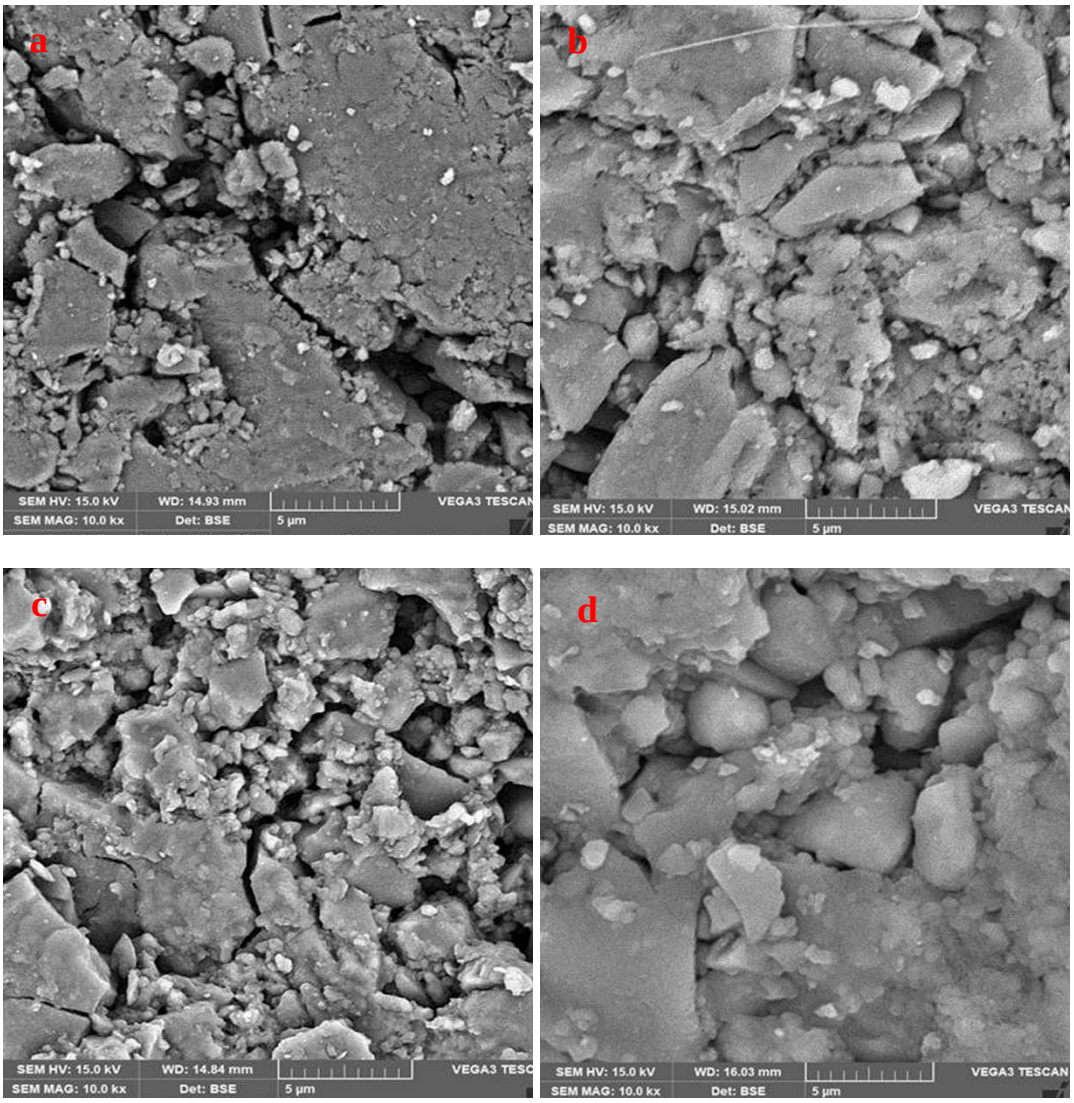

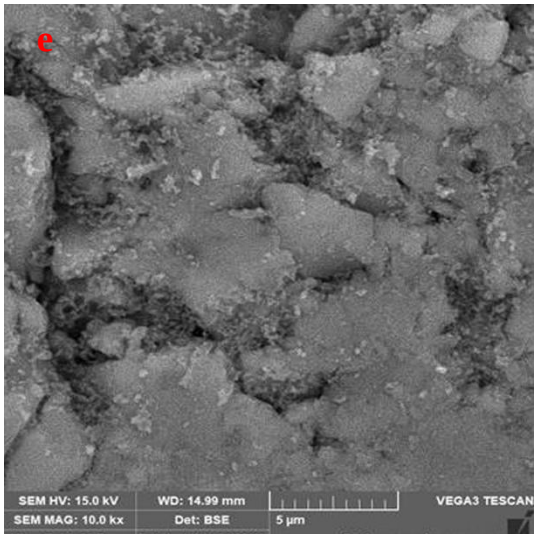

Figure 4. The scanning electron microscopy (SEM) images of the samples with different calcination temperatures (a) 200ºC, (b) 250ºC., (c) 300ºC., (d) 400ºC and (d) 450ºC

Table 1. Element Composition of samples according to EDX spectra

Calcination (ºC)	Oxygen O (wt%)	Carbon C (wt%)	Silicon Si (wt%)	Sulfur S (wt%)	Sodium Na (wt%)
200	40.60	50.96	7.63	0.81	-
250	42.47	46.34	9.71	1.18	0.30
300	41.57	45.86	11.68	0.89	-
400	41.62	42.66	13.86	1.37	0.49
450	42.53	37.50	17.68	1.51	0.78

The microstructure of the sample (Fig 4a) displays quite different characteristics to those of the samples with temperature of calcination 250, 300, 400 and 450 ºC (Fig 4(b-e)). The EDS data presented in Table 1clearly indicated the significant effect of the increase temperature of calcination on the composition of the samples. As can be seen, the sample (Fig 4a) contained a very large amount (50.96 %) of C, and the percentage of this element decreased to 37.50 % in the sample with increase temperature of calcination up to 450 ºC. Meanwhile, the sample with temperature of calcination 200 ºC contained 7.63% of Si and increased to 17.68 % with the increase temperature of calcination up to 450 ºC. The surfaces of the samples (Fig 4b-d) are marked by fine grains of silica structure cover several large grains of asphalt structure, which according to XRD results (Fig. 2(a-d)) are composed of carbon and silica amorph. The presence of carbon and silica phases in the last four samples suggest that increase of calcination temperature led to decomposition of asphalt may be due to by the asphalt-compatible fractions spread homogenously in a continuous asphalt phase as a result of the increase calcination temperature. Furthermore, the SEM image indicates that the sample is denser with calcination temperature of 450, which leads to a compact shape in accordance with the results of compressive strength analyses, described in the following section.

3.3 Physical characteristic of silica-asphalt composite

Figure 5 shows the changes in density and porosity of the samples as a function of calcination temperatures. As can be observed in Fig. 5, the density of the calcined samples increases slowly up to 300, while the porosity of the calcined samples decrease slowly as the calcination temperatures increase up to 250 °C, and beyond this temperature, relatively sharply lines of the two characteristics were observed up to 450 °C calcination temperature. As shown in Fig. 5, the densities of the calcined samples increase from 2.4 to 4.1 g/cm^3 as the calcination temperature increased from 200 to 450 °C. The porosity was sharply decreased up to 450 °C. The sharp increase of the density with increasing temperature up to 450 °C, followed by a sharp decrease of the porosity with increasing temperature from 250 to 450 °C, was attributed to the increased amount of silicon as displayed by the EDX results presented in Table 1. The change in density was most likely due to reacting of carbon and silica as displayed by the XRD results presented in Fig. 2.

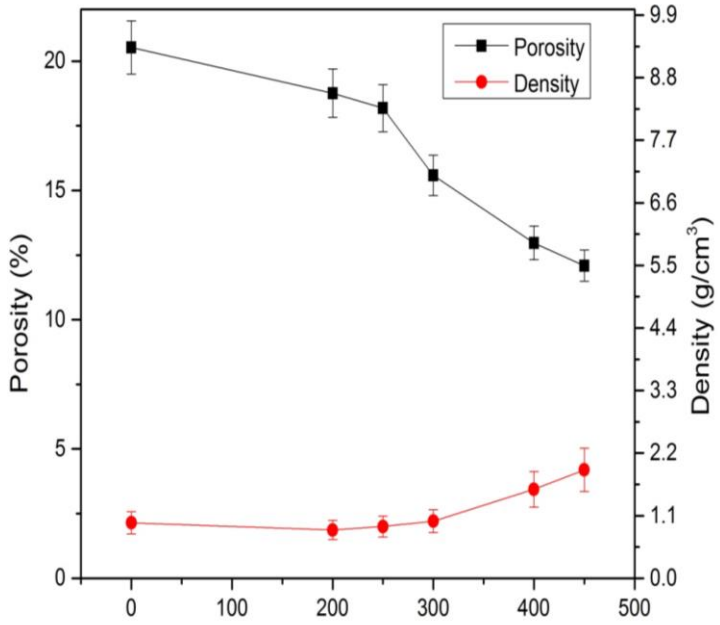

Figure 5. Variation of porosity and density of the samples with different calcination temperatures

The effect of the thermal treatments on the compressive strength is shown in Figure 7. The result indicates that the compressive strength of the silica asphalt composite increased with increasing calcination temperatures, followed by decreased slowly up to 450 °C. As shown in Figure 7, the compressive strength increased sharply with increasing the calcination temperatures up to 300 °C . The sharp increase in the compressive strength with the increasing the calcination temperatures up to 300 °C referred to the increase in the density and the decrease in the porosity as shown in Figure 5. The compressive strength increased with the calcination temperatures increasing from 200 to 300 °C, and reached the value of 42.5 MPa at the calcination temperature of 450 °C. This trend implies that the samples became highly compact and dense as a result of the increased amount of silica and the decreased amount of carbon (Table 1).

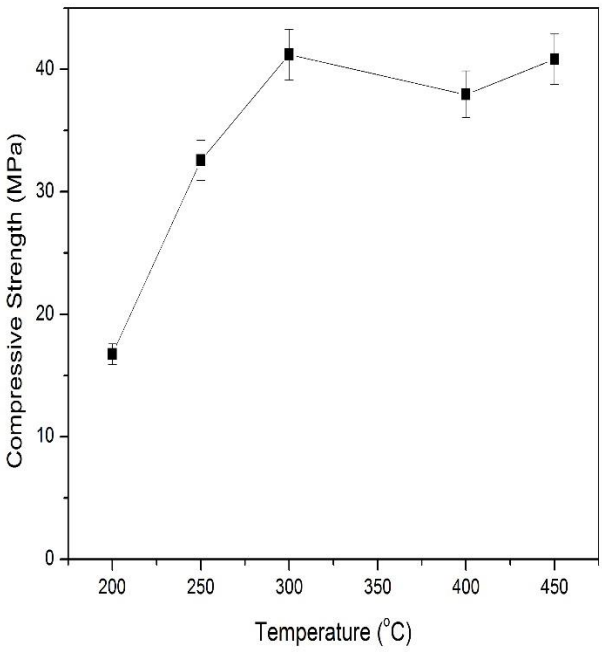

Figure 6. Variation of compressive strength of the samples of the samples with different calcination temperatures(a) 200°C, (b) 250°C., (c) 300 °C., (d) 400°C and (d) 450°C

4. Conclusions

This study demonstrated that asphalt composite was successfully prepared using rice husk silica as raw material by thermal treatments. The XRD study revealed that the major phases were carbon and silica amorphous, which were associated with are Si-OH, Si-O-Si and C-H functional groups according to FTIR analysis. In addition, an increased calcination temperature was followed by an increase in the density and compressive strength. Also, the result presents that the asphalt composite with calcination temperature of 300 °C is suitable for the design of roof materials with highest compressive strength value. Based on these characteristics, the samples are considered for the roof material, suggesting their potential use in substitute lightweight steel roof devices.

Acknowledments

The authors wish to thank and appreciate Ministry of Research, Technology, and High Education, Directorate General of Strengthening Research and Development, Republic of Indonesia for research funding provided through *the Decentralization Research/*Basic research university/*PDUPT Grant*: /UN26/KU/2020.

References

[1] Saleh, M.F. (2004). New Zealand Experience with Foam Bitumen Stabilization, *Journal of Transport Research Board*,1868, 40-49.

[2] Fawcett A.H. and Lort, S.K. (2003). Structure Formation in Polymeric Fibers, *Journal of Polymer*, 29,1992.

[3] Wei, H.B., Li, Z.Q and Jiao, Y.B. (2017). Effects of diatomite and SBS on freeze-thaw resistance of crumb rubber modified asphalt mixture, *Advances in Materials Science and Engineering*, 1-14.

[4] Cao, K. Xu, W., Chen D., and Feng H., (2018). High- and Low-Temperature Properties and Thermal Stability of Silica Fume/SBS Composite-Modified Asphalt Mortar, *Advances in Materials Science and Engineering*, 1-8, doi.org/10.1155/2018/1317436.

[5] Yang, Y and Cheng, Y., (2016). Preparation and performance of asphalt compound modified with waste crumb rubber and waste polyethylene, *Advances in Materials Science and Engineering*, 1-6.

[6] Gonzalez, V., Martinez, B. and Navarro, F.J. (2010). Thermo-mechanical properties of bitumen modified with crumb tire rubber and polymeric additives, *Journal of fuel processing Technology*, 91,1033-1039.

[7] Naskar, M., Chaki, T.K. and Reddy, K.S. (2010). Effect of waste plastic as modifier on thermal stability and degradation kinetics of bitumen/waste plastic blend, *Journal of thermochimica act*, 509,128-134.

[8] Fang, C.Q., Jiao, L.N. and Huetal, J.B. (2014). Viscoelasticity of asphalt modified with packaging waste expended polystyrene, *Journal of Materials Science and Technology*, 30, 939-943.

[9] Hinislioglu S. and Agar E. (2004). Use of waste high density polyethylene as bitumen modifier in asphalt concrete mix, *Materials Letters*, 58, 267–271.

[10] Francisco, J., Pedro, P. and Martinez, B. (2010). Novel recycled polyethylene/ground tire rubber/ bitumen blends for use in roofing applications: Thermo-mechanical properties, *Journal of Polymer testing;* 29:588-595.

[11] Zhang, F. and Yu, J.Y. (2010). The research for high-performance SBR compound modified asphalt, *Construction and Building Materials*, 24, 410-418.

[12] Wang, H., You, Z.P., Mills-Beale, J.L. and Hao, P.W. (2012). Laboratory evaluation on high temperature viscosity and low temperature stiffness of asphalt binder with high percent scrap tire rubber, *Construction and Building Materials*, 26, 583-590.

[13] Arabani, M., Mirabdolazimi, S.M. and Sasani, A.R. (2010). The effect of waste tire thread mesh on the dynamic behaviour of asphalt mixtures, *Construction and Building Materials*, 24,1060-1068.

[14] Ngoc, N.N., Le Xuan, T., La The, V., Bui Thi, V.A. (2018), High-purity amorphous silica from rice husk: Preparation and characterization, *Vietnam Journal of Chemistry*, 56(6), 730-736, doi.org/10.1002/vjch.201800079

[15] Khopthong, W and Cherdhirunkorn, B. (2020). Production of silica-based ceramics sintered under nitrogen atmosphere from rice husk and sugarcane bagasse ash, *Journal of Metals, Materials and Minerals*, 30 (2), 76-82.

[16] Shen, J., Liu, X., Zhu, S., Zhang, H., Tan, J. (2011). Effects of calcination parameters on the silica phase of original and leached rice husk ash, *Materials Letters*, 65(8), 1179-1183, doi: 10.1016/j.matlet.2011.01.034.

[17] Chandrasekhar, S., Pramada, P.N., and Majeed, J. (2006). Effect of calcination temperature and heating rate on the optical properties and reactivity of rice husk ash, *Journal of Materials Science*, 41, 7926–7933. doi: 10.1007/s10853-006-0859-0.

[18] Lee, L., C. Zeng, X. Cao, X. Han and J. Shen J. (2005). Polymer nanocomposite foams. Composites Science Technology, 65, 2344-2363. doi: 10.1016/j.compscitech.2005.06.016.

[19] Sembiring, S., Situmeang, R., Sembiring, Z. (2019), Synthesis and characterization of asphalt composite precursors using amorphous rice husk silica, *Cerâmica*, 65, 194-199, doi:10.1590/0366-69132019653742497.

[20] Sembiring, S., Riyanto, A., Situmeang, R., Sembiring, Z. (2019). Bituminous Composite Comprising Amorphous Silica from Rice Husks, *Ceramics-Silikáty* 63 (3), 277-286 (2019), doi: 10.13168/cs.2019.0021.

[21] P. L. Cong, P.L., S. F. Chen, S.F. and H. X. Chen, H.X. (2012). Effects of diatomite on the properties of asphalt binder, *Construction and Building Materials*, 30, 495–499.

[22] Y. Song, Y., J. Che, J. and Y. Zhang, Y. (2011). The interacting rule of diatomite and asphalt groups, *Petroleum Science and Technology*, 29 (3), 254–259.

[23] Ping, L., and Yunlong, L. (2014). Review on Nano Modified Asphalt. *Applied Mechanics and Materials*, *587*, 1220.

[24] Tan, Y.Q., Shan, L.Y. and Fang, J. (2009). Anti-cracking mechanism of diatomite asphalt and diatomite asphalt mixture at low temperature, *Journal of Southeast University*, 25 (1),74-78.

[25] Abutalib, N., Fini, E.H., Aflaki, S and Abu-Lebdeh, T.M, (2015). Investigating Effects of Application of Silica Fume to Reduce Asphalt Oxidative Aging, *American Journal of Engineering and Applied Sciences*, 8 (1), 176.184 doi: 10.3844/ajeassp.2015.176.184.

[26] Kai, C., Xu, W., Chen, D. and Huimin, F. (2018). High- and low-temperature properties and thermal stability of silica fume/SBS composite-modified asphalt mortar, *Advances in Materials Science and Engineering*, 1-8.

[27] Li, C., Wu, S., Tao, G., Xiao, Y., (2018). Initial Self-Healing Temperatures of Asphalt Mastics Based on Flow Behavior Index, *Materials*, 11, 917.

[28] Vila-Cortavitarte, M., Jato-Espino, D., Castro-Fresno, D., Calzada-Pérez, M.Á., (2018). Self-Healing Capacity of Asphalt Mixtures Including By-Products Both as Aggregates and Heating Inductors, *Materials*, 11, 800.

[29] Karol, M.S., Kowalski, J., Jan B. Król, B. and Radziszewski, P. (2019). Influence of Overheating Phenomenon on Bitumen and Asphalt Mixture Properties, *Materials*, 12 (610) 1-19, doi:10.3390/ma12040610www.

[30] Singh, S.K., Kumar, Y., Ravindranath, S.S., (2018). Thermal degradation of SBS in bitumen during storage: Influence of temperature, SBS concentration, polymer type and base bitumen. *Polymer Degradation Stability*. 147, 64-75.

[31] Sembiring, S., Simanjuntak, W., Manurung, P., Asmi, D. and Low, I.M. (2014). Synthesis and characterisation of gel-derived mullite precursors from rice husk silica. *Ceramic International*, 40, 7067-7072.

[32] Sembiring, S., Riyanto, A., Simanjuntak, W. and Situmeang, R. (2017). Effect of MgO-SiO_2 ratio on the forsterite (Mg_2SiO_4) precursors characteristics derived from amorphous rice husk silica, *Journal of Oriental Chemistry*, 33,186-192.

[33] Sembiring, S., Simanjuntak, W., Situmeang, R., Riyanto, A. and Sebayang, K. (2016). Preparation of refractory cordieirite using amorphous rice husk silica for thermal insulation purposes, *Ceramic International*, 42, 8431-8437.

[34] Amutha, K., Ravibaskar, R. and Sivakumar, G. (2016). Extraction, synthesis and characterization of nano silica from rice husk ash. *International nano Technology and Application*, 4, 61-66.

[35] Tuan, L.N.A., Dung, L.T.K., Ha, L.D.T., Hien, N.Q., Phu, D.V., Du, B.D. (2017). Preparation and characterization of nano silica from rice husk ash by chemical treatment combined with calcination. *Vietnam Journal of Chemistry*, vol. 55, pp. 446-455.

[36] Liou T.H. and Yang, C.C. (2011). Synthesis and surface characteristics of nano silica produced from alkali-extracted rice husk ash. *Material Science Enggineering*, B 176, 521-529.

[37] Carmona, V.B., Oliveira, R.M., Silva, W.T.L., Mattoso, L.H.C. and Marconcini, J.M. (2013). Nano silica from rice husk: extraction and characterization," *Industry Crops and Production*, 43, 291-296.

[38] Mohamed, M.M., Zidan, F.I. and Thabet, M. (2008). Synthesis of ZSM-5 zeolite from rice husk ash: characterization and implications for photocatalytic degradation catalysts," *Micropore and Mesopore Material*, 108, 193-203.

[39] Zahra, G. and Habibollah, Y. (2011). Preparation and characterization of nano zeolite NaA from rice husk at room temperature without organic additives. *Nano Material*, 1-8.

[40] Mehta, A and Ugwekar, R.P. (2015). Extraction of silica and other related products from rice husk, *International Engineering Research and Application*, 25, 43-48.

[41] Xu, H., Gao, B., Cao, H., Chen, X., Yu, L., Wu, K., Sun, L., Peng, X and Fu, J. (2014). Nano porous activated carbon derived from rice husk for high performance super capacitor," *Nano Material*, 1-7.

[42] Andreola, F., Martín, M.I., Ferrari, A.M., Lancellotti, I., Bondioli, J.M. Rincón, M. Romero and L. Barbieri (2013). Technological properties of glass-ceramic tiles obtained using rice husk ash as silica precursor, *Ceramic International*, 39, 5427–5435.

[43] Australian Standard, Refractories and Refractory Material Physical Test Methods (1989). The Determination of Density, Porosity and Water Adsorption, Australian Standard (1-4); 1774.

[44] JIS A 5908. (2003). Japanese Standard Association. Japanesse Industrial Standard Particle Board JIS A 5908. Japanese Standard Association.

[45] Sankar, S., Sharma, S.K., Kaur, N., Lee, B., Kim, D.Y., Lee, S., Jung, H. (2016). Biogenerated silica nano particles synthesized from sticky, red, and brown rice husk ashes by chemical method, *Ceramics International*, 42,4875-4885.

[46] Le Nghiem, A.T., Lai Thi, K.D., Le Doan T.H., Nguyen Q.H., Dang, V.P., Bui D.D. (2017). Preparation and characterization of nano silica from rice husk ash by chemical treatment combined with calcination, *Vietnam Journal of Chemistry International* Edition,55(4): 455-459, doi: 10.15625/2525-2321.2017-00490.

[47] Feng, Q., Chen, K., Ma, D. (2018). Synthesis of high specific surface area silica aerogel from rice husk ash via ambient pressure drying. *Colloids and Surfaces*, A539:399-406.

[48] Bathla, A., Narula1, C., Chauhan, R.P. (2018). Hydrothermal synthesis and characterization of silica nanowires using rice husk ash: an agricultural waste. *Journal of Materials Science: Materials in Electronics*, 29, 6225–6231.

[49] Zhang F., Yu J., Han J. (2011). Effects of thermal oxidative ageing on dynamic viscosity, TG/DTG, DTA and FTIR of SBS- and SBS/sulfur-modified asphalts. *Construction and Building Materials, 25*(1), 129-137. doi:10.1016/j.conbuildmat.2010.06.048.

[50] Yao H., Dai Q., You Z. (2015). Fourier Transform Infrared Spectroscopy characterization of aging-related properties of original and nano-modified asphalt binders. *Construction Building Material, 101*(1), 1078-1087. doi: 10.1016/j.conbuildmat.2015.10.085.

[51] Ouyang C., Wang S., and Zhang Y. (2006). Improving the aging resistance of asphalt by addition of Zinc dialkyldithiophosphate. *Fuel, 85* (7-8), 1060-1066. doi: 10.1016/j. *fuel*.2005.08.023.

[52] Larsen D.O., Alessandrini J.L., Bosch A., and Cortizo M.S. (2009). Micro-structural and rheological characteristics of SBS-asphalt blends during their manufacturing. *Construction and Building Materials, 23*(8), 2769-2774. doi: 10.1016/j.conbuildmat.2009.03.008.